Role of calcium ions on the removal of haloacetic acids from swimming pool water by nanofiltration: mechanisms and implications

Linyan Yang [a,b], Jin Zhou [c,d], Qianhong She [e], Man Pun Wan [f], Rong Wang [c,e], Victor W.-C. Chang *[,b,c], Chuyang Y. Tang *[,g]

[a] Interdisciplinary Graduate School, Nanyang Technological University, 50 Nanyang Avenue, Singapore 639798, Singapore

[b] Residues and Resource Reclamation Centre (R3C), Nanyang Environment and Water Research Institute, Nanyang Technological University, 1 Cleantech Loop, CleanTech One, Singapore 637141, Singapore

[c] Division of Environmental and Water Resources, School of Civil and Environmental Engineering, Nanyang Technological University, 50 Nanyang Avenue, Singapore 639798, Singapore

[d] Singapore-Berkeley Building Efficiency and Sustainability in the Tropics (SinBerBEST) program, Berkeley Education Alliance for Research in Singapore (BEARS) Center, Singapore

[e] Singapore Membrane Technology Centre (SMTC), Nanyang Environment and Water Research Institute, Nanyang Technological University, 1 Cleantech Loop, CleanTech One, Singapore 637141, Singapore

[f] School of Mechanical and Aerospace Engineering, Nanyang Technological University, 50 Nanyang Avenue, Singapore 639798, Singapore

[g] Department of Civil Engineering, University of Hong Kong, Pokfulam, Hong Kong

Corresponding Authors

*Phone: +65-67904773; fax: +65-67921650; e-mail: wcchang@ ntu.edu.sg (V.W.C.C.).

*Phone: +852-28591976; fax: +852-25595337; e-mail: tangc@ hku.hk (C.Y.T.).

Abstract

We investigated the removal of haloacetic acids (HAAs) from swimming pool waters (SPWs) by two nanofiltration membranes NF270 and NF90. The strong matrix effect (particularly by Ca^{2+}) on membrane rejection prompts us to systematically investigate the mechanistic role of Ca^{2+} in HAA rejection. At typical SPW pH of 7.5, NF90 maintained consistently high rejection of HAAs (> 95%) with little influence by Ca^{2+}, thanks to the dominance of size exclusion effect for this tight membrane (pore radius ~ 0.31 nm). In contrast, the rejections of both inorganic ions (e.g., Na^{+} and Cl^{-}) and HAA anions were decreased at higher Ca^{2+} concentration for NF270 (pore radius ~ 0.40 nm). Further tests show that the rejection of neutral hydrophilic molecular probes and the membrane pore size were not affected by Ca^{2+}. Although Ca^{2+} is unable to form strong complex with HAAs, we observed the binding of Ca^{2+} to NF270 together with a reduction in its surface charge. Therefore, the formation of membrane-Ca^{2+} complex, which weakens charge interaction effect, was responsible for the reduced HAA rejection. The current study reveals important mechanistic insights of the matrix effect on trace contaminant rejection, which is critical for a better understanding of their fate and removal in membrane-based treatment.

Keywords: Haloacetic acids; Membranes; Matrix effect; Calcium; Swimming pool water

1. Introduction

Haloacetic acids (HAAs) exist widely in a variety of water environments, e.g. wastewater, drinking water, ground water and swimming pool water (SPW), mainly attributed to the use of chlorination for water disinfection. As a group of known disinfection by-products (DBPs), HAAs have raised public concerns due to their potential genotoxicity and carcinogenicity (Richardson et al., 2007). United States Environmental Protection Agency (US EPA) therefore has regulated a maximum contaminant level (MCL) of 60 μg/L for the sum of five HAAs for drinking water (EPA, 1998). Our recent survey shows that HAA concentrations in typical SPWs reach more than an order of magnitude higher than the MCL in drinking water (Yang et al., 2016a). Other researchers have also reported high HAA concentrations in pools in the U.S. and Germany (Stottmeister and Naglitsch, 1996; Wang et al., 2014). Therefore the potential health problem becomes a big challenge for swimmers exposed in SPWs with high HAAs.

Membrane technology has been used as an effective method for the removal of trace contaminants, e.g. DBPs, pharmaceuticals, pesticides, and hormones (Doederer et al., 2014; Nghiem et al., 2004; 2005; Simon et al., 2013). Good rejection of HAAs has been achieved (≥ 90%) by either nanofiltration (NF), reverse osmosis (RO), or forward osmosis (FO) in the context of drinking water and wastewater treatment (Chalatip et al., 2009; Kimura et al., 2003; Kong et al., 2014). In a previous study, we reported the use of NF/RO for the removal of HAAs in a simple electrolyte solution (50 mM NaCl at pH 7.5) and demonstrated that the rejection was attributed to combined effects of size exclusion and charge repulsion. A unified approach has been developed to quantify the rejection based on the physical-chemical properties of the

membranes and solutes (Yang et al., 2016b). Nevertheless, real SPWs can be far more complicated (Table 1) and the matrix effect on the rejection of HAAs has yet to be systematically studied. In particular, calcium ions present commonly in SPWs as a second most abundant cation only after sodium ions, with a typical concentration of ~ 0.5 mM in Singapore pools and up to ~2 mM in other pools (Buczkowska-Radlinska et al., 2013). Compared to other common ions (e.g., Na^+, K^+, Mg^{2+}, Cl^-) in SPWs, Ca^{2+} possesses a greater potential to affect membrane performance, attributing to its stronger ability to interact with a variety of solutes as well as membrane materials (Ahn et al., 2008). In the context of membrane fouling, the role of Ca^{2+} has been well documented (Tang et al., 2011). Ca^{2+} can form complexes with certain ligand groups (e.g., $-COO^-$) of proteins, polysaccharides, and natural organic matters, leading to charge neutralization and bridging effects with typically increased fouling tendency (Ang and Elimelech, 2008; Hong and Elimelech, 1997; Tang et al., 2007b; van den Brink et al., 2009; Yoon et al., 1998). It has also been reported that Ca^{2+} can significantly alter the surface properties of polyamide membranes by binding to the carboxylic groups contained in these membranes (Herzberg et al., 2009; Jin et al., 2009; Mi and Elimelech, 2010; Motsa et al., 2014). On the other hand, only a handful of studies have systematically examined the effect of Ca^{2+} on trace contaminant removal by membranes (Mahlangu et al., 2014; Zhao et al., 2013).

The coexistence of HAAs and Ca^{2+} in typical SPW matrix arouses the necessity to explore the HAA removal from SPWs containing Ca^{2+}, which has seldom been investigated. Presumably, Ca^{2+} can interact either with HAAs or membranes (e.g., by binding to the carboxylic groups to form HAA-Ca^{2+} or membrane-Ca^{2+} complex) therefore altering the rejection behaviour. We were therefore prompted to investigate

96 the effect of Ca^{2+} on HAA removal systematically. We analysed the rejection of 9
97 HAAs together with 7 surrogate molecules by two commercial NF membranes (NF90
98 and NF270) in order to resolve the underlying mechanisms involved with respect to
99 the role of Ca^{2+} in trace contaminant rejection. The fundamental mechanistic
100 understanding will provide deeper insights for further extending of the membrane
101 technology for the SPW treatment.
102
103 ## 2. Materials and methods
104 ### 2.1 Chemicals and materials
105 **HAAs.** Nine HAAs were used in this study, including chloroacetic acid (CAA),
106 bromoacetic acid (BAA), dichloroacetic acid (DCAA), bromochloroacetic acid
107 (BCAA), dibromoacetic acid (DBAA), trichloroacetic acid (TCAA),
108 bromodichloroacetic acid (BDCAA), dibromochloroacetic acid (DBCAA) and
109 tribromoacetic acid (TBAA) (Supporting Information S1). All of them were
110 purchased from Sigma-Aldrich in analytical grades with ≥ 97% purity. A stock
111 solution containing a mixture of 1 g/L of each HAA was prepared by dissolving the
112 pure chemicals in MilliQ water (Millipore, Billerica, MA). Reagents used for HAA
113 quantification were of GC grades for solvents (e.g. methyl tert-butyl ether (MTBE)
114 and methanol) and of at least ACS grades for other chemicals (e.g. 98% sulfuric acid,
115 sodium bicarbonate, copper sulfate and sodium sulfate).
116
117 **Surrogate compounds.** Glycerol, erythritol, xylose, glucose, maltose, sucrose and
118 raffinose were of analytical grades with purity over 99%. Sucrose was purchased from
119 United States Biochemical (USB) and the others were from Sigma-Aldrich. These
120 neutral hydrophilic compounds were used as additional probe molecules for resolving

the mechanisms involved in solute rejection by membranes. A mixture of 40 g/L of each surrogate molecule was prepared with MilliQ water as the stock solution.

Other chemicals. Sodium chloride and calcium chloride were with purity over 99% from Merck. Sodium hydroxide and hydrochloric acid (37%) used for pH adjustment were at least analytical grade. Potassium bromide (Sigma, 99%), lithium chloride (ACROS, anhydrous, 99%), boric acid (ACS, ISO, Ph Eur, Merck, 99.5-100.5%), sodium nitrate (Sigma, ACS, >99.0%), sodium sulfate (Sigma, granular, ACS, >99%) and urea (Ph Eur, ACS, Merck) were used for the preparation of synthetic SPW. Real SPWs were collected from a public outdoor pool disinfected by sodium hypochlorite in the campus of Nanyang Technological University, Singapore. The major criteria for the synthetic SPW are: 1) synthetic SPW had a similar ionic strength to the real SPW, and an intermediate pH value of 7.5 based on the regulated pH range of 7.20-7.80 for SPW context by National Environment Agency (NEA), Singapore; 2) major ions in the synthetic SPW had similar concentrations to those in the real SPW (with the exception that higher concentrations were adopted for components with high detection limits to facilitate our analysis, see Table 1); 3) constituents that may cause membrane scaling (e.g., Fe and Al) or interact with calcium ions (organic carbon species, e.g., citric acid) were omitted. The synthetic SPW was prepared in accordance to Supporting Information S2.

NF membranes. Two commercial NF membranes were investigated in this study, including a fully aromatic polyamide membrane NF90 and a semi-aromatic polyamide membrane NF270 (Dow Filmtec) (Tang et al., 2009a; b). The physiochemical properties of these two membranes have been characterized in our

prior study (Yang et al., 2016b) and are summarized in Table 2. Compared to the loose NF270, NF90 is a tighter nanofiltration membrane characterized with its higher NaCl rejection, smaller molecular weight cut-off (MWCO) and pore radius, as well as lower water permeability.

2.2 Membrane characterization

Zeta potential. The zeta potential of the membrane surface was measured by a SurPASS electrokinetic analyzer (Anton Paar GmbH, Graz, Austria). The channel height of 100-150 μm was maintained between two adjustable gap cells (20 × 10 mm). Two pieces of virgin membranes were attached to each cell with face-to-face orientation. The 50 mM NaCl solution was used as a background electrolyte and the solution pH was manually adjusted to 7.5 by 1 M NaOH. In order to assess the effect of Ca^{2+} on the membrane surface charge, a predetermined volume of a 0.1 M $CaCl_2$ solution was manually pipetted to achieve a Ca^{2+} concentration over the range of 0 to 1 mM. Experiments showed that a 10-min stirring by an electromagnetic agitator was enough for solution stabilization. Then the measurement was conducted twice for the same membrane coupon, and totally 4 values were obtained for each condition. The average zeta potential was calculated based on the Helmholtz-Smoluchowski (HS) equation (Chun et al., 2003).

Contact angle. The contact angle of membranes was measured by a Goniometer (DataPhysics, OCA 15EC). The dried membrane samples were attached to a glass slide by a double-sided tape to ensure a flat membrane surface before measurement. The contact angle of each sample was measured for at least 10 times at different

locations. The average and standard deviation were obtained by discarding the maximum and minimum values (Table 2).

XPS analysis. The elemental composition of the material from the top 0 to 5 nm of the surface region can be determined by X-ray photoelectron spectroscopy (XPS, Thermo Scientific Escalab 250Xi) with a detection limit of 0.1%. The Ca^{2+} binding to the membrane surface was quantified by XPS analysis, following the sample preparation procedures proposed by Do et al. (2012). Briefly, the virgin membranes were thoroughly rinsed and soaked in the MilliQ water for 24 h. They were then immersed in $CaCl_2$ solutions (e.g., 0.1, 1 mM, and 0 mM as a control) with pH adjustment to 7.5 by 0.1 mM HCl or NaOH for 60 min. The membranes were then rinsed with 0.001 mM $CaCl_2$ solution (at pH 7.5) for 4 times to remove the Ca^{2+} that was not binded to the membrane surface. The membranes were dried in vacuum before XPS analysis.

2.3 Membrane filtration experiments

Membrane setup. A bench scale cross-flow membrane filtration setup (Supporting Information S3) was used in this study. The details for the setup and filtration protocol were elaborated in our previous work (Yang et al., 2016b) and briefly described as follows. The filtration system contains four parallel cross-flow CF042 cells (an effective area of 42 cm^2 and a channel size of 4.6 × 9.2 cm, Delrin Acetal, Sterlitech, Kent, WA, USA). A spacer (GE Osmonics, Minnetonka, MN, USA) of 1.2 mm thickness was placed in each cell for the filtration tests. A chiller (Polyscience, Niles, IL, USA) was used to control the temperature of feed solution at 25 ºC.

Filtration experiments. Before the filtration tests, the virgin membranes (after being soaked for 24 h in the MilliQ water) were loaded into the cell. The permeate and retentate circulated back to the feed tank to maintain the feed concentration constant. For all filtration tests, the applied pressure, cross-flow and solution temperature were kept at 100 psi, 2.4 L/min (corresponding to 54.3 cm/s cross-flow velocity) and 25 ºC, respectively. To minimize the effect of membrane compaction, all membrane coupons were filtered for 24 h in the feed solutions before sample collection for analysis.

Rejection of ionic species was measured for both real and synthetic SPWs (Table 1). The HAA rejection tests (100 μg/L of each HAA in the feed) were conducted for synthetic SPW. The total HAA concentration (sum of nine HAAs) in real and synthetic SPW was comparable (1002 v.s. 900 μg/L, as shown in Table 1). The solution pH was adjusted to 7.5 by dosing 1 M NaOH or HCl and measured by a portable pH meter (Mettler Toledo, SevenGo pro). An additional solution pH of 3.5 for HAA rejection tests was also included for comparison purpose. The solution pH did not show significant variation during the experiment. To study the effect of Ca^{2+}, $CaCl_2$ stock solution (0.1 or 1 M) was added to the feeds to achieve a predetermined Ca^{2+} concentration over the range of 0 to 1 mM. The same membrane coupon was used for different Ca^{2+} concentrations to diminish the minor material difference of different regions. The filtration setup was run for 1 h at each Ca^{2+} concentration to ensure system stabilization, after which both feed and permeate were collected for analysis. Surrogate rejection tests were performed using a feed solution containing 200 mg/L of each surrogate at pH 7.5. Background electrolytes were not added in the surrogate rejection tests to avoid its interference with the surrogate analysis by HPLC-RID.

220

221 ## 2.4 Analytical methods

222 **HAA quantification.** HAAs were quantified based on a modified EPA 552.3 method
223 proposed by Yang et al. (2016a). This method involved three key steps: 1) liquid-
224 liquid extraction by solvent MTBE; 2) derivatization of HAAs by acidic methanol (10%
225 sulfuric acid in methanol); 3) analysis of methylated HAAs by GCMS (GC: Agilent
226 7890B; MS: Agilent 5977A; column: DB-5MS (J & W Scientific, 5% phenyl - 95%
227 dimethyl polysiloxane, 30 m × 0.25 mm ID, 0.25 μm film thickness)). The detection
228 limit of individual HAA was 2 μg/L. The flow chat of HAA analysis procedure is
229 shown in Supporting Information S4.

230

231 **Surrogate quantification.** High-performance liquid chromatography coupled with
232 refractive index detector (HPLC-RID, Agilent 1260 Infinity) has been demonstrated
233 as an effective technique to quantify these surrogates (Yang et al., 2016b). The
234 columns used were Hi-Plex Pb (7.7 × 300 mm, 8 μm, guard)/(7.7 × 50 mm, 8 μm,
235 analytical). The detection limit of each surrogate was 1 mg/L. The detailed
236 information for this analysis was described elsewhere (Yang et al., 2016b).

237

238 **Elemental quantification.** The elements, including Na, Ca, K, Mg, Fe, Mn, Cu, Sr,
239 Zn, Li, Al, and B, were measured by an inductively coupled plasma - optical emission
240 spectrometry (ICP-OES, PerkinElmer, UK) for concentrations with the level of
241 milligram per liter and/or by an inductively coupled plasma - mass spectroscopy (ICP-
242 MS) for concentrations with the level of microgram per liter. The anions, including F,
243 Cl, NO_2, NO_3, SO_4, PO_4, and Br, were determined by an ion chromatography (IC,
244 Dionex ICS-1100 with autosampler Dionex AS-HV). Ammonia ions were determined

by chromogenic reactions based on the salicylate method detected by a portable DR 2800 spectrophotometer (Hach, USA). Total organic carbon (TOC) and total nitrogen (TN) were measured by a TOC_N analyzer (multi N/C®2100S, Analytikjena, Germany). Urea was determined based on the enzymatic and colorimetric indophenol blue method (Microquant® urea test; from Merck) by a UV/Vis-Spectrophotometer (Cary 50, Agilent) under a wavelength of 690 nm with a calibration range of 0.1-10 mg/L (Supporting Information S5). The detection limit of each compound is shown in Table 1.

3. Results and discussion

3.1. Properties of real SPWs

The characteristics of a typical real SPW are shown in Table 1. The concentrations of individual HAA and the sum of nine HAAs in real SPW are shown in Supporting Information S1 and Table 1. Chlorinated HAAs (e.g., dichloroacetic acid, trichloroacetic acid) turned out to be the main components in this chlorinated pool. Sodium and chloride ions are two predominant species (~ 50 mM) in SPWs, which control the solution ionic strength and lead to the high conductivity (~ 5 ms/cm). The circulated SPW treatment system might cause the accumulation of the salinity, which contains two sources, body fluid (e.g., sweat and urine) released from the bathers and chemicals (e.g., NaClO for disinfection and HCl for pH adjustment) dosed for water purification (Zwiener et al., 2007). In addition to Na^+, other cations (e.g., Ca^{2+}, K^+, Mg^{2+}) were commonly detected in SPW matrix with a concentration level of milligram per liter. Remarkably, among these cations Ca^{2+} turned out to be a second most abundant ion with a concentration of ~ 0.5 mM, which mainly comes from the

filling tap water (Ca^{2+} in tap water is similar to that in SPWs according to our preliminary experiment).

3.2. Rejection of inorganic solutes by membranes

3.2.1. Real SPW

The rejection of inorganic components in real SPWs was measured for both NF270 (Figure 1A) and NF90 (Figure 1B). The rejection data demonstrated two remarkable trends: 1) neutral compounds, e.g. boron, had low rejections (< 30%) by both membranes; 2) the rejection of charged ionic species increased dramatically with the increased valence state for both cations and anions. For NF270 (Figure 1A), the maximum rejections of monovalent ions reached ~ 50%, while those for divalent ions were in the range of 55 to nearly 100%. These results reveal the important role of electrostatic interaction for NF membranes, which is in good agreement with other literature studies (Bartels et al., 2005; Childress and Elimelech, 2000; Su et al., 2006).

NF90 demonstrated a similar rejection trend of higher rejection for ions with greater valence state (Figure 1B). Compared to NF270, NF90 had consistently higher rejection. In addition, the rejection data for NF90 were less scattered. NF90 had a smaller average pore radius of 0.31 nm, which implies a more important role of size exclusion for this membrane compared to NF270 (pore radius of 0.40 nm). The current study confirms the importance of both electrostatic interaction and size exclusion on membrane rejection.

3.2.2. Comparing real and synthetic SPWs

293 Figure 1C compares the rejection of different species in real and synthetic SPWs for
294 NF270, where the synthetic SPW was dosed either 0 or 0.5 mM Ca^{2+}. The significant
295 variations in the rejection values observed under the three different solution
296 conditions reveal the critical role of matrix effect for NF270. In particular, the
297 addition of 0.5 mM Ca^{2+} into the synthetic SPW reduced the rejection of most ionic
298 species significantly. In contrast, the matrix effect was much less obvious for the
299 tighter membrane NF90 that experiences a stronger size exclusion effect (Figure 1D).
300 The synthetic SPW filtration by NF90 and NF270 over a wider Ca^{2+} concentration
301 range of 0-1 mM (Supporting Information S6) further supports these observations.
302 The ubiquitous presence of Ca^{2+} in SPWs and its great influence on membrane
303 rejection behaviour prompt us to conduct a systematic evaluation of the mechanistic
304 role of Ca^{2+} in rejecting HAAs in SPWs (Section 3.3).
305

306 ## 3.3. Rejection of HAAs by membranes

307 ### *3.3.1. Effect of Ca^{2+} on HAA rejection*

308 Figure 2A,B show the effect of Ca^{2+} on HAA rejection by NF270 and NF90,
309 respectively. To avoid the overcrowding of the figures, HAAs were grouped into
310 mono-halogenated (MHAAs), di-halogenated (DHAAs), and tri-halogenated acetic
311 acids (THAAs) based on the number of halogen atoms. HAA rejection by NF90 (>
312 95%) was not significantly affected by the degree of halogenation or the addition of
313 Ca^{2+}. This observation can be attributed to the dominant role of size exclusion: the
314 radii of HAAs range from 0.21-0.27 nm and are nearly comparable to the pore radius
315 of NF90 (0.31 nm) (Yang et al., 2016b). On the contrary, the rejection by the looser
316 NF270 membrane (pore radius of 0.40 nm) followed the order of MHAAs < DHAAs
317 < THAAs, which correlates well with the degree of halogenation (or equivalently the

molecular size) (Yang et al., 2016b). Increasing Ca^{2+} concentration from 0 to 1 mM caused the membrane rejection to decrease by approximately 20%. The effect of Ca^{2+} on the rejection of HAAs is consistent with that on the rejection of inorganic species reported in Section 3.2.

The precipitation of HAAs in the presence of Ca^{2+} was eliminated as HAA concentration in the feed water kept nearly constant with the addition of Ca^{2+} throughout the experiment (data not shown). The effect of Ca^{2+} on membrane rejection can be potentially attributed to its interaction with either HAAs or membrane surface. Both HAAs and the polyamide NF membranes contain carboxylic groups ($-COO^-$), which provide ligand sites for binding with Ca^{2+} (Herzberg et al., 2009; Jin et al., 2009; Mi and Elimelech, 2010; Motsa et al., 2014). Accordingly, three distinct mechanisms are plausible (Figure 2C): 1) the formation of HAA-Ca^{2+} complex, resulting in reduced charge density of HAAs together with a change in the size of the dissolved species (HAA-Ca^{2+} induced effect); 2) the formation of membrane-Ca^{2+} complex, which affects the pore size of the membrane (membrane-Ca^{2+} induced size exclusion effect); and 3) the formation of membrane-Ca^{2+} complex, which results in a partial neutralization of membrane surface charge (membrane-Ca^{2+} induced charge interaction effect). These mechanisms are further resolved through Section 3.3.2-3.3.4.

3.3.2. HAA-Ca^{2+} induced effect

Figure 3 shows the potential formation of HAA-Ca^{2+} complex on the basis of the following chemical speciation analysis,

$$CR_3COOH = CR_3COO^- + H^+,\ K_a = \frac{[CR_3COO^-]\cdot[H^+]}{[CR_3COOH]} \quad (1)$$

$$CR_3COO^- + Ca^{2+} = CR_3COOCa^+,\ K_1 = \frac{[CR_3COOCa^+]}{[CR_3COO^-]\cdot[Ca^{2+}]} \quad (2)$$

where CR_3COO^- represents an HAA anion (-R = -H, -Cl, or -Br), and K_a and K_1 are the acidity constant and stability constant, respectively. The bridging of two HAA molecules by Ca^{2+} (e.g., $(CR_3COO)_2Ca$) is not considered due to the relatively low HAA concentrations (~ or <1 μM, Supporting Information S1). As indicated in Figure 3, the two MHAAs (chloroacetic acid and bromoacetic acid) exist predominantly in their anionic forms (only < 0.2% as $CH_2ClCOOCa^+$ and < 0.4% as $CH_2BrCOOCa^+$ for Ca^{2+} concentration up to 1 mM). Compared to acetic acid, HAAs have smaller pK_a values (Supporting Information S1) as a result of the strong electron withdrawing effect of the halogen atoms, leading to a weaker binding with H^+ (Reusch, 2013; Stumm and Morgan, 2012). Similarly, HAAs had weaker binding with Ca^{2+} as indicated by their smaller $\log K_1$ compared to that of acetic acid (data from NIST database). Despite that the stability constants for DHAAs and THAAs are not available in the literature, their abilities to form HAA-Ca^{2+} complex are even weaker as more halogens further reduce the charge density of $–COO^-$ and therefore reduce the binding energy between Ca^{2+} and HAA anions. Therefore, the mechanism of HAA-Ca^{2+} complex formation is inadequate to explain the rejection behaviour presented in Figure 2.

3.3.3. Membrane-Ca^{2+} induced size exclusion effect

Early studies have reported that the membrane pore size can be potentially affected by the solution chemistry (Childress and Elimelech, 2000). To determine whether Ca^{2+} can lead to a change in the membrane pore size, we performed rejection tests of seven surrogate molecules (glycerol, erythritol, xylose, glucose, maltose, sucrose, and

raffinose) over a Ca^{2+} concentration range of 0-1 mM. The neutral hydrophilic nature of these surrogate compounds has allowed their use as molecular probes for determining membrane pore size (Nghiem et al., 2004) and for assessing the size exclusion effect (Yang et al., 2016b). Ca^{2+} did not have a significant effect on the rejection of the surrogates for both NF270 (Figure 4A) and NF90 (Figure 4B). The membrane permeate water flux also maintained nearly constant over the entire Ca^{2+} concentration range (Supporting Information S7). Accordingly, the average pore size of the membranes, calculated in accordance to Nghiem et al. (2004), was not affected by the presence of Ca^{2+} (Figure 4C). Therefore, the mechanism of membrane-Ca^{2+} induced size exclusion effect is unable to explain the reduced HAA rejection at higher Ca^{2+} concentration (Figure 2A).

3.3.4. Membrane-Ca^{2+} induced charge interaction effect

Figure 5A demonstrates that both membrane surfaces became less negatively charged with the increasing Ca^{2+} concentrations, supporting our hypothesis that Ca^{2+} affects the membrane rejection by altering their surface charge properties (Figure 2C). Yoon et al. (2005) and Childress and Elimelech (1996) also found that Ca^{2+} possesses a much stronger charge neutralization ability compared to other electrolytes, e.g., KCl, K_2SO_4 and Na_2SO_4, attributed to its stronger binding to the membrane surface. The binding of Ca^{2+} to membrane surface is further supported by our XPS analysis, with much intense calcium signals detected for the membranes exposed to 0.1 and 1 mM Ca^{2+} compared to the control (no Ca^{2+}) (Figure 5B-D). It can be explained by the interaction between Ca^{2+} and the ligand groups (particularly $-COO^-$) (Herzberg et al., 2009; Jin et al., 2009; Mi and Elimelech, 2010; Motsa et al., 2014). Indeed, Ca^{2+} binding has been used to characterize the relative abundance of $-COO^-$ groups

contained in polyamide membranes (Do et al., 2012). In the current study, the effect of Ca^{2+} on zeta potential was more considerable for NF270 than NF90, which is attributed to the greater presence of $-COO^-$ groups in NF270.

3.3.5. Combined effects of size exclusion and charge interaction on HAA rejection

To further assess the role of size exclusion and charge interaction, we measured HAA rejections by NF270 at pH 3.5 with or without Ca^{2+}. At pH 3.5, the membrane is nearly neutral (Yang et al., 2016b). In addition, the saturation of carboxylic groups with H^+ (i.e., -COOH instead of $-COO^-$) prevents the binding of Ca^{2+} to the membrane. Therefore, this pH condition effectively suppresses the charge interaction and thus establishes a baseline case of the size exclusion effect. A plot of HAA rejection at pH 3.5 as a function of the molecular radius (Figure 6) indicates an increased rejection that benefited from the enhanced size exclusion for the bulkier molecules (with molecular radius increased from ~ 0.21 to ~ 0.27 nm). The presence of Ca^{2+} did not significantly affect the HAA rejection at this low pH (also see Supporting Information S8) since Ca^{2+} is outcompeted by H^+ for binding to the membrane ligand sites.

In the absence of Ca^{2+}, increasing pH from 3.5 to 7.5 dramatically enhanced the HAA rejection from 30-55% to > 80%. Compared to the near-neutral membrane surface at pH 3.5 (zeta potential ~ -5 mV (Yang et al., 2016b)), NF270 became highly negatively charged at pH 7.5 (zeta potential ~ -36 mV (Yang et al., 2016b)). Thus, the difference in rejection between pH 3.5 and pH 7.5 characterizes the effect of charge interaction on HAA removal. This difference became larger at a lower molecular radius, which indicates that charge interaction has to assume a more predominant role for the smaller molecules (in the presence of weaker size exclusion). Similarly, HAA

rejection has a stronger dependence on the size exclusion effect when there was a weaker charge interaction, as reflected by the steeper slope of the rejection curve at pH 3.5 compared to that at pH 7.5.

The HAA rejection at pH 7.5 with 1 mM Ca^{2+} was significantly lower than that at the same pH without Ca^{2+}. Nevertheless, it was still substantially higher than that at pH 3.5 (or $[H^+]$ = 0.32 mM). The current study shows that both Ca^{2+} and H^+ decreased HAA rejection by binding to the carboxylic groups on the membrane, though H^+ had a more severe effect by completely neutralizing the membrane surface charge at pH 3.5.

3.4. Implications

As discussed in Section 3.3.1-3.3.4, the membrane-Ca^{2+} induced charge interaction effect is the main mechanism that contributes to the reduced rejection of HAAs and inorganic ions (e.g., Na^+ and Cl^-) in the presence of Ca^{2+}. To further consolidate this conclusion, we simulated the conductivity rejection (same as Cl^- and Na^+) by a transport model developed by Bowen et al. (1997), only considering the changed membrane surface charge in the presence of Ca^{2+} (see Supporting Information S9 and S10). The good fitness between measured and simulated conductivity rejection confirms the reduced rejection is due to the neutralization effect of Ca^{2+} on membrane surface charge.

It is worthwhile to note that the polyamide membranes used in the current study are not tolerant to chlorine. Therefore, the presence of chlorine in SPWs has to be adequately addressed. One possibility is to use chlorine tolerant membranes (e.g., see

441 Klüpfel et al. (2011)). These membranes typically have much lower water
442 permeability compared to polyamide-based nanofiltration membranes, which implies
443 significantly higher energy consumption. An alternative way is to include a chlorine
444 removal step before membrane treatment (similar to the practice in seawater
445 desalination) to protect the downstream polyamide membranes. It is further possible
446 to apply periodical NF treatment to minimize the chemical dosage for
447 chlorination/dechlorination. The cost-benefit of these approaches needs to be further
448 studied. The current study used urea as a model organic compound in the synthetic
449 SPW. Real SPWs also contain other organic matters, e.g., creatinine, uric acid, citric
450 acid, etc., from swimmers' body fluid and some natural organic matters (mainly
451 humic and fulvic acids) from the source water, which are normally quantified as TOC
452 in total (Yang et al., 2016a). Future studies shall systematically investigate their role
453 in HAA removal by membranes (e.g., through membrane fouling). For example, the
454 co-presence of dissolved organic matter and divalent cations (calcium and magnesium)
455 may lead to severe organic fouling (Tang et al., 2007a); the enhanced concentration
456 polarization in the cake layer may result in reduced solute rejection (Hoek and
457 Elimelech, 2003; Tang et al., 2011). The modification of surface properties by the
458 fouling layer and the foulant-solute interactions can further alter the membrane
459 rejection behavior (Steinle-Darling and Reinhard, 2008; Yoon et al., 1998; Zhao et al.,
460 2016). Therefore, these additional potential matrix effects need to be further
461 addressed.
462

463 **4. Conclusions**

464 Membrane filtration has the high potential to achieve good HAA removal efficiency.
465 For the tight NF90 membrane whose pore size is comparable to HAAs, their rejection

was consistently high (>95%) and was not significantly affected by the water matrix, reflecting the dominance of size exclusion effect. However, the HAA rejection by loose NF270 membrane at pH 7.5 was significantly reduced at increased concentration of calcium, a commonly detected ion in SPWs. This matrix effect can be attributed to the formation of membrane-Ca^{2+} complex (as shown by the XPS results) and the resulting partial charge neutralization of the membrane surface (supported by the zeta potential measurements). In contrast, the rejection of neutral hydrophilic molecular probes was not affected by the presence of Ca^{2+}, suggesting that the formation of membrane-Ca^{2+} complex did not affect the pore structure of the membrane. Thus, it was the weakened charge interaction, instead of size exclusion, that was responsible for the reduced rejection of HAAs in the case of NF270. The fundamental understanding of this matrix effect on contaminant rejection promotes the effective application of membrane technology to practical SPW treatment.

Supporting information

S1. Properties of haloacetic acids (HAAs) and surrogate molecules; S2. Characteristics of synthetic swimming pool water (SPW); S3. Schematic diagram of the membrane filtration setup; S4. Flow chart of HAA analysis procedure; S5. Urea calibration; S6. Effect of calcium ions on rejections of neutral compounds, cations, and anions; S7. Effect of calcium ions on water flux; S8. Effect of calcium ions on HAA rejection at pH 3.5 by NF270; S9. Comparison of measured and simulated conductivity rejection in the presence of calcium ions; S10. Transport model for charged ions.

Acknowledgements

Yang Linyan receives the scholarship from Interdisciplinary Graduate School (IGS) at Nanyang Technological University (NTU), Singapore. The authors also acknowledge Residues and Resource Reclamation Centre (R3C), Nanyang Environment and Water Research Institute (NEWRI) for the laboratory support.

References

Ahn, W.-Y., Kalinichev, A.G., Clark, M.M., 2008. Effects of background cations on the fouling of polyethersulfone membranes by natural organic matter: experimental and molecular modeling study. Journal of Membrane Science 309 (1–2), 128-140.

Ang, W.S., Elimelech, M., 2008. Fatty acid fouling of reverse osmosis membranes: Implications for wastewater reclamation. Water Research 42 (16), 4393-4403.

Bartels, C., Franks, R., Rybar, S., Schierach, M., Wilf, M., 2005. The effect of feed ionic strength on salt passage through reverse osmosis membranes. Desalination 184 (1–3), 185-195.

Bowen, W.R., Mohammad, A.W., Hilal, N., 1997. Characterisation of nanofiltration membranes for predictive purposes—use of salts, uncharged solutes and atomic force microscopy. Journal of Membrane Science 126 (1), 91-105.

Buczkowska-Radlinska, J., Lagocka, R., Kaczmarek, W., Gorski, M., Nowicka, A., 2013. Prevalence of dental erosion in adolescent competitive swimmers exposed to gas-chlorinated swimming pool water. Clinical Oral Investigations 17 (2), 579-583.

Chalatip, R., Chawalit, R., Nopawan, R., 2009. Removal of haloacetic acids by nanofiltration. Journal of Environmental Sciences 21 (1), 96-100.

Childress, A.E., Elimelech, M., 1996. Effect of solution chemistry on the surface charge of polymeric reverse osmosis and nanofiltration membranes. Journal of Membrane Science 119 (2), 253-268.

Childress, A.E., Elimelech, M., 2000. Relating nanofiltration membrane performance to membrane charge (electrokinetic) characteristics. Environmental Science & Technology 34 (17), 3710-3716.

Chun, M.-S., Lee, S.-Y., Yang, S.-M., 2003. Estimation of zeta potential by electrokinetic analysis of ionic fluid flows through a divergent microchannel. Journal of Colloid and Interface Science 266 (1), 120-126.

Do, V.T., Tang, C.Y., Reinhard, M., Leckie, J.O., 2012. Effects of chlorine exposure conditions on physiochemical properties and performance of a polyamide membrane-mechanisms and implications. Environmental Science & Technology 46 (24), 13184-13192.

Doederer, K., Farré, M.J., Pidou, M., Weinberg, H.S., Gernjak, W., 2014. Rejection of disinfection by-products by RO and NF membranes: influence of solute properties and operational parameters. Journal of Membrane Science 467, 195-205.

EPA, U., 1998. National primary drinking water regulations: disinfectants and disinfection byproducts; final rule. 63, 69390–69476.

Herzberg, M., Kang, S., Elimelech, M., 2009. Role of extracellular polymeric substances (EPS) in biofouling of reverse osmosis membranes. Environmental Science & Technology 43 (12), 4393-4398.

Hoek, E.M., Elimelech, M., 2003. Cake-enhanced concentration polarization: a new fouling mechanism for salt-rejecting membranes. Environmental Science & Technology 37 (24), 5581-5588.

Hong, S., Elimelech, M., 1997. Chemical and physical aspects of natural organic matter (NOM) fouling of nanofiltration membranes. Journal of Membrane Science 132 (2), 159-181.

Jin, X., Huang, X., Hoek, E.M., 2009. Role of specific ion interactions in seawater RO membrane fouling by alginic acid. Environmental Science & Technology 43 (10), 3580-3587.

Kimura, K., Amy, G., Drewes, J.E., Heberer, T., Kim, T.-U., Watanabe, Y., 2003. Rejection of organic micropollutants (disinfection by-products, endocrine disrupting compounds, and pharmaceutically active compounds) by NF/RO membranes. Journal of Membrane Science 227 (1), 113-121.

Klüpfel, A.M., Glauner, T., Zwiener, C., Frimmel, F.H., 2011. Nanofiltration for enhanced removal of disinfection by-product (DBP) precursors in swimming pool water–retention and water quality estimation. Water Science and Technology 63 (8), 1716-1725.

Kong, F.-x., Yang, H.-w., Wang, X.-m., Xie, Y.F., 2014. Rejection of nine haloacetic acids and coupled reverse draw solute permeation in forward osmosis. Desalination 341, 1-9.

Mahlangu, T.O., Hoek, E.M.V., Mamba, B.B., Verliefde, A.R.D., 2014. Influence of organic, colloidal and combined fouling on NF rejection of NaCl and carbamazepine: role of solute-foulant-membrane interactions and cake-enhanced concentration polarisation. Journal of Membrane Science 471, 35-46.

Mi, B., Elimelech, M., 2010. Organic fouling of forward osmosis membranes: fouling reversibility and cleaning without chemical reagents. Journal of Membrane Science 348 (1–2), 337-345.

Motsa, M.M., Mamba, B.B., D'Haese, A., Hoek, E.M.V., Verliefde, A.R.D., 2014. Organic fouling in forward osmosis membranes: the role of feed solution chemistry and membrane structural properties. Journal of Membrane Science 460, 99-109.

Nghiem, L.D., Schäfer, A.I., Elimelech, M., 2004. Removal of natural hormones by nanofiltration membranes: measurement, modeling, and mechanisms. Environmental Science & Technology 38 (6), 1888-1896.

567 Nghiem, L.D., Schäfer, A.I., Elimelech, M., 2005. Pharmaceutical retention mechanisms by
568 nanofiltration membranes. Environmental Science & Technology 39 (19), 7698-7705.
569 Reusch, W., 2013. Carboxylic Acids.
570 https://www2.chemistry.msu.edu/faculty/reusch/virttxtjml/crbacid1.htm.
571 Richardson, S.D., Plewa, M.J., Wagner, E.D., Schoeny, R., Demarini, D.M., 2007.
572 Occurrence, genotoxicity, and carcinogenicity of regulated and emerging disinfection
573 by-products in drinking water: a review and roadmap for research. Mutation research
574 636 (1-3), 178-242.
575 Simon, A., McDonald, J.A., Khan, S.J., Price, W.E., Nghiem, L.D., 2013. Effects of caustic
576 cleaning on pore size of nanofiltration membranes and their rejection of trace organic
577 chemicals. Journal of Membrane Science 447 (0), 153-162.
578 Steinle-Darling, E., Reinhard, M., 2008. Nanofiltration for Trace Organic Contaminant
579 Removal: Structure, Solution, and Membrane Fouling Effects on the Rejection of
580 Perfluorochemicals. Environmental Science & Technology 42 (14), 5292-5297.
581 Stottmeister, E., Naglitsch, F., 1996. Human exposure to other disinfection by-products than
582 trihalomethanes in swimming pools. Annual report of the Federal Environmental
583 Agency, Berlin, Germany (in German).
584 Stumm, W., Morgan, J.J. (2012) Aquatic chemistry: chemical equilibria and rates in natural
585 waters, John Wiley & Sons.
586 Su, M., Wang, D.-X., Wang, X.-L., Ando, M., Shintani, T., 2006. Rejection of ions by NF
587 membranes for binary electrolyte solutions of NaCl, NaNO3, CaCl2 and Ca(NO3)2.
588 Desalination 191 (1–3), 303-308.
589 Tang, C.Y., Chong, T.H., Fane, A.G., 2011. Colloidal interactions and fouling of NF and RO
590 membranes: a review. Advances in Colloid and Interface Science 164 (1–2), 126-143.
591 Tang, C.Y., Kwon, Y.-N., Leckie, J.O., 2007a. Characterization of humic acid fouled reverse
592 osmosis and nanofiltration membranes by transmission electron microscopy and
593 streaming potential measurements. Environmental Science & Technology 41 (3),
594 942-949.
595 Tang, C.Y., Kwon, Y.-N., Leckie, J.O., 2007b. Fouling of reverse osmosis and nanofiltration
596 membranes by humic acid-effects of solution composition and hydrodynamic
597 conditions. Journal of Membrane Science 290 (1), 86-94.
598 Tang, C.Y., Kwon, Y.-N., Leckie, J.O., 2009a. Effect of membrane chemistry and coating
599 layer on physiochemical properties of thin film composite polyamide RO and NF
600 membranes: I. FTIR and XPS characterization of polyamide and coating layer
601 chemistry. Desalination 242 (1), 149-167.
602 Tang, C.Y., Kwon, Y.-N., Leckie, J.O., 2009b. Effect of membrane chemistry and coating
603 layer on physiochemical properties of thin film composite polyamide RO and NF

membranes: II. Membrane physiochemical properties and their dependence on polyamide and coating layers. Desalination 242 (1), 168-182.

van den Brink, P., Zwijnenburg, A., Smith, G., Temmink, H., van Loosdrecht, M., 2009. Effect of free calcium concentration and ionic strength on alginate fouling in cross-flow membrane filtration. Journal of Membrane Science 345 (1-2), 207-216.

Wang, X., Leal, M.G., Zhang, X., Yang, H., Xie, Y., 2014. Haloacetic acids in swimming pool and spa water in the United States and China. Frontiers of Environmental Science & Engineering, 1-5.

Yang, L., Schmalz, C., Zhou, J., Zwiener, C., Chang, V.W.C., Ge, L., Wan, M.P., 2016a. An insight of disinfection by-product (DBP) formation by alternative disinfectants for swimming pool disinfection under tropical conditions. Water Research 101, 535-546.

Yang, L., She, Q., Wan, M.P., Wang, R., Chang, V.W.-C., Tang, C.Y., 2016b. Removal of haloacetic acids from swimming pool water by reverse osmosis and nanofiltration (under review).

Yoon, S.-H., Lee, C.-H., Kim, K.-J., Fane, A.G., 1998. Effect of calcium ion on the fouling of nanofilter by humic acid in drinking water production. Water Research 32 (7), 2180-2186.

Yoon, Y., Amy, G., Yoon, J., 2005. Effect of pH and conductivity on hindered diffusion of perchlorate ions during transport through negatively charged nanofiltration and ultrafiltration membranes. Desalination 177 (1–3), 217-227.

Zhao, C., Tang, C.Y., Li, P., Adrian, P., Hu, G., 2016. Perfluorooctane sulfonate removal by nanofiltration membrane—the effect and interaction of magnesium ion/humic acid. Journal of Membrane Science 503, 31-41.

Zhao, C., Zhang, J., He, G., Wang, T., Hou, D., Luan, Z., 2013. Perfluorooctane sulfonate removal by nanofiltration membrane the role of calcium ions. Chemical Engineering Journal 233, 224-232.

Zwiener, C., Richardson, S.D., De Marini, D.M., Grummt, T., Glauner, T., Frimmel, F.H., 2007. Drowning in disinfection byproducts? Assessing swimming pool water. Environmental Science & Technology 41 (2), 363-372.

Table 1 Characteristics of swimming pool water

	Unit	Analytical instrument	Real SPW[a]	Synthetic SPW[b]	Detection limit
Na	mg/L	ICP-OES	1062±90	1175	0.1
Ca			19.2±5.0	0 (40)	0.1
K			15.7±0.3	20	0.1
Mg			0.5±0.2		0.1
Fe	µg/L	ICP-MS	68.4±6.0		0.5
Mn			0.2±0.3		0.5
Cu			3.4±3.9		0.5
Sr			37.1±5.7		0.5
Zn			0.3±0.3		0.5
Li			1.2±0.2	100[c]	0.5
Al			38.0±24.5		0.5
B			65.6±22.2	100	0.5
F	mg/L	IC	<0.2		0.2
Cl			1953±71	1775 (1864)	1
NO_2			<1		1
NO_3			20.8±1.0	20	1
SO_4			58.0±12.0	60	1
PO_4			<2		2
Br			<1	41[c]	1
NH_4		DR 2800 Spectrophotometer	0.1±0.1		0.02
TOC		TOC/TN	1.7±0.3		1
TN			5.1±0.1		1
Urea			0.23±0.19	10[c]	0.1
Free chlorine[d]		UV/Vis-Spectrophotometer	0.57 ± 0.75		0.05
Combined chlorine[d]			0.06 ± 0.03		
HAAs[d]	µg/L	GCMS	1002 ± 216	900	
pH		pH meter	7.9±0.1[e]	7.5[e]	
Conductivity	ms/cm	Conductivity meter	4.98		
Ionic strength	mM		53	52 (55)	

Notes:

[a] Mean ± standard deviation (n=4).

[b] The synthetic SPW was under the background condition of 50 mM NaCl and the addition of Ca^{2+} up to 40 mg/L by $CaCl_2$ increased chloride concentration to 1864 mg/L and ionic strength to 55 mM.

[c] Concentrations in synthetic SPW were higher than the realistic values due to the high detection limit of analytical methods

[d] Data from Yang et al. (2016a).

[e] The pHs measured in real SPWs were a bit higher than the range 7.2-7.8 regulated by NEA, Singapore. Therefore, we used pH 7.5 in synthetic SPW to simulate the ideal pool conditions.

Table 2 Membrane properties (Data were extracted from Yang et al. (2016b), except RMS roughness from Tang et al. (2009) and contact angle by this study)

Membrane	Surface layer material	Manufacturer	Water permeability[a]	Nominal NaCl rejection[b]	MWCO[c]	ζ potential at pH 7.5[d]	Pore radius[e]	RMS roughness	Contact angle
			L/m^2 h bar	%	Da	mV	nm	nm	°
NF90	Fully aromatic polyamide	Dow Filmtec	7.69	82.7	118	-33	0.31 (0.31[f])	142.8±9.6	54.1±2.6
NF270	Semi- aromatic polyamide	Dow Filmtec	16.10	30.6	266	-36	0.40 (0.44[f])	9.0±4.2	26.5±1.7

[a] Water permeability was obtained by compacting the membranes for 24 h under the defined conditions (100 psi, 25 °C, pH ~6.7, MilliQ water).

[b] NaCl rejection was determined after NaCl was dosed to the feed tank for 24 h under defined conditions (100 psi, 25 °C, pH ~6.7, 50 mM NaCl).

[c] MWCOs were obtained using neutral hydrophilic compounds as the probing molecules.

[d] Zeta potential was evaluated at pH 7.5 with 50 mM NaCl as the background electrolyte.

[e] Pore radius was calculated by a solute transport model in accordance to Nghiem et al. (2004).

[f] The calculated pore radius of NF270 was 0.40 nm, which was slightly smaller compared to the value reported in our previous study (0.44 nm). The slight difference may arise from the different batches of membrane materials. The calculated pore radius of NF90 was identical in two studies.

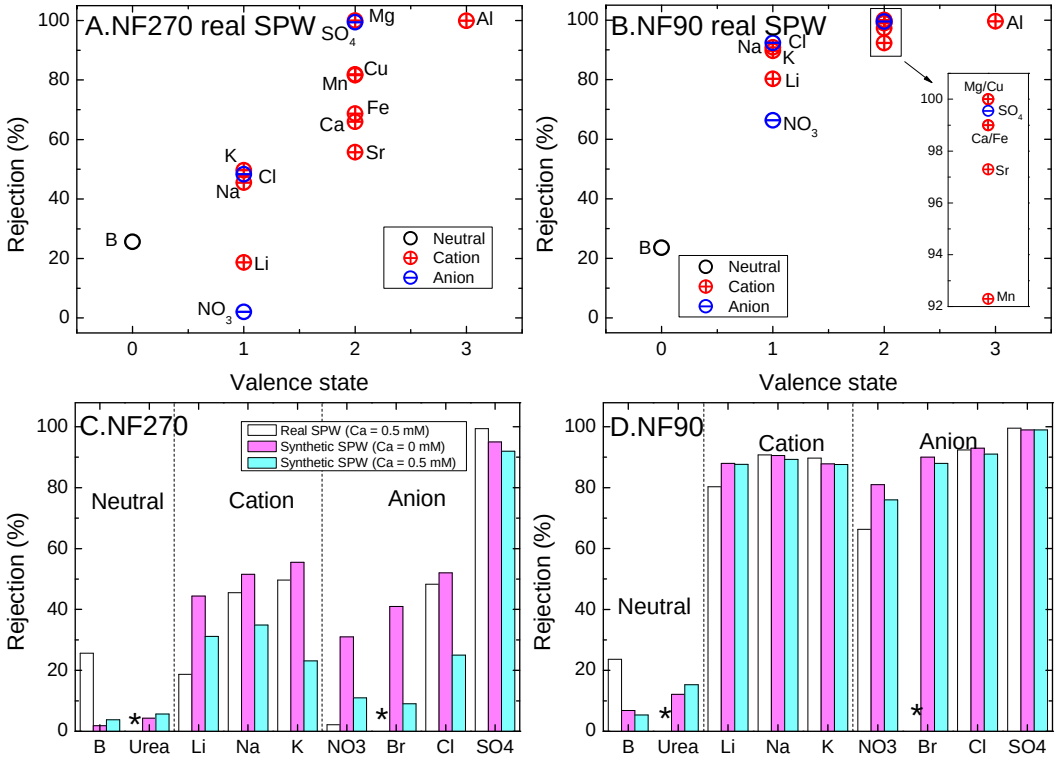

Figure 1 The rejection of components in real and synthetic SPWs by NF270 and NF90. * The rejection data for urea in real SPW was not available and bromide ion in real SPW was not detectable (<1 mg/L).

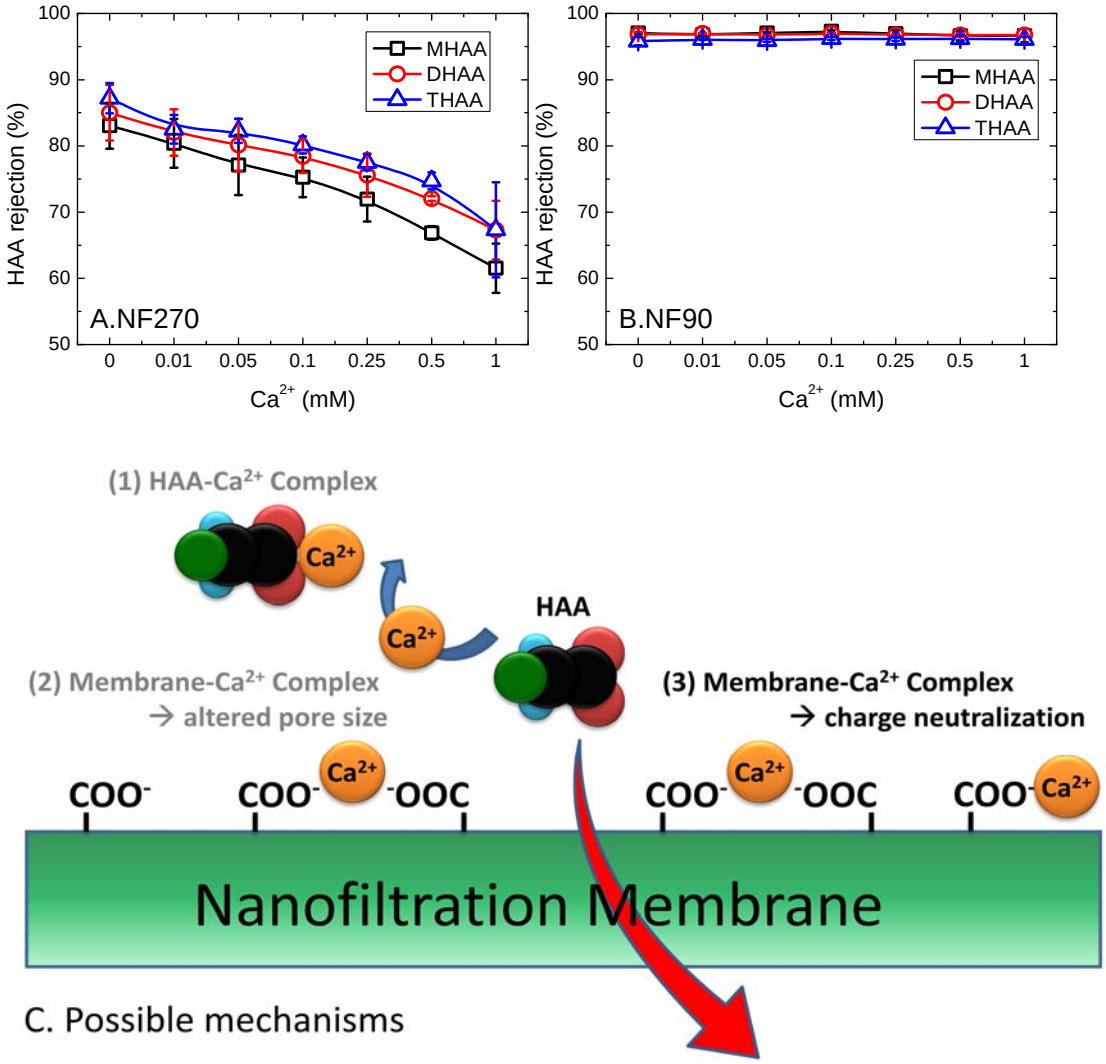

Figure 2 Effect of calcium ions on HAA rejection. Rejection data for NF270 (A) and NF90 (B) using synthetic SPW at pH 7.5. A conceptual diagram (C) illustrates the three possible mechanisms involved (1. HAA-Ca^{2+} induced effect; 2. membrane-Ca^{2+} induced size exclusion effect; and 3 membrane-Ca^{2+} induced charge interaction effect). The error bars represent the range based on two independent experiments.

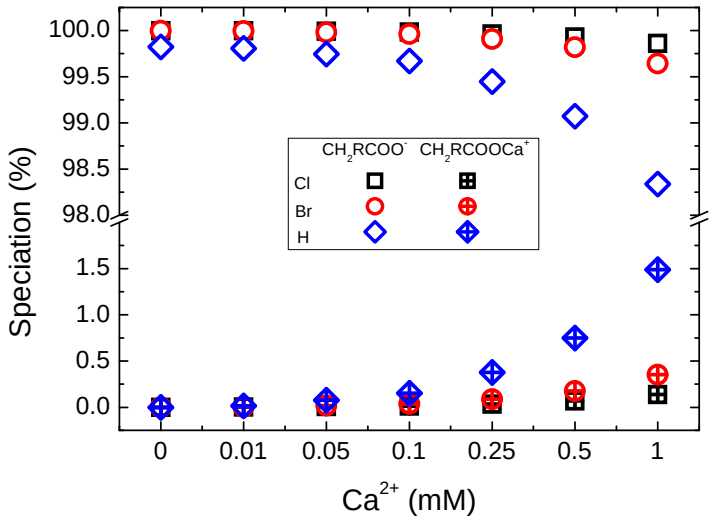

Figure 3 Species distribution of chloroacetic acid, bromoacetic acid, and acetic acid in the presence of calcium ions. The log values of stability constants for calcium-based complexes are 0.14, 0.55, and 1.18, respectively.

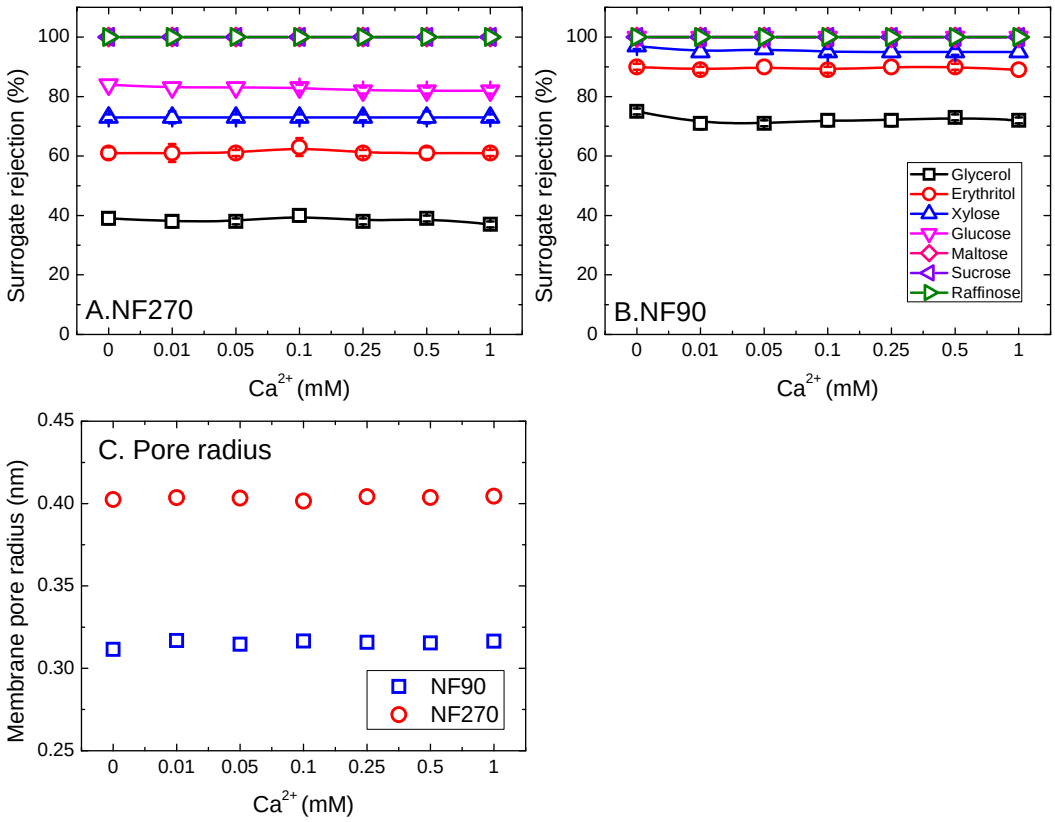

Figure 4 Effect of calcium ions on surrogate rejection by NF270 (A) and NF90 (B), and membrane pore size (C) calculated in accordance to Nghiem et al. (2004). The error bars represent the range based on two independent experiments.

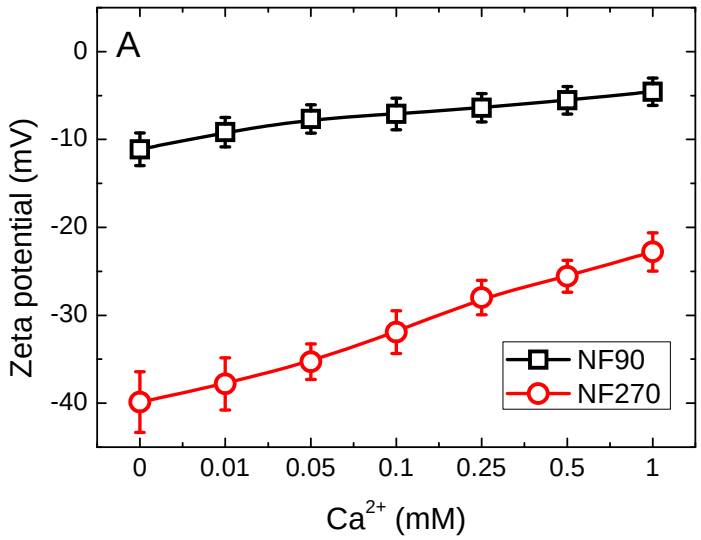
A
Zeta potential (mV)
0
-10
-20
-30
-40
NF90
NF270
0
0.01
0.05
0.1
0.25
0.5
1
Ca2+ (mM)

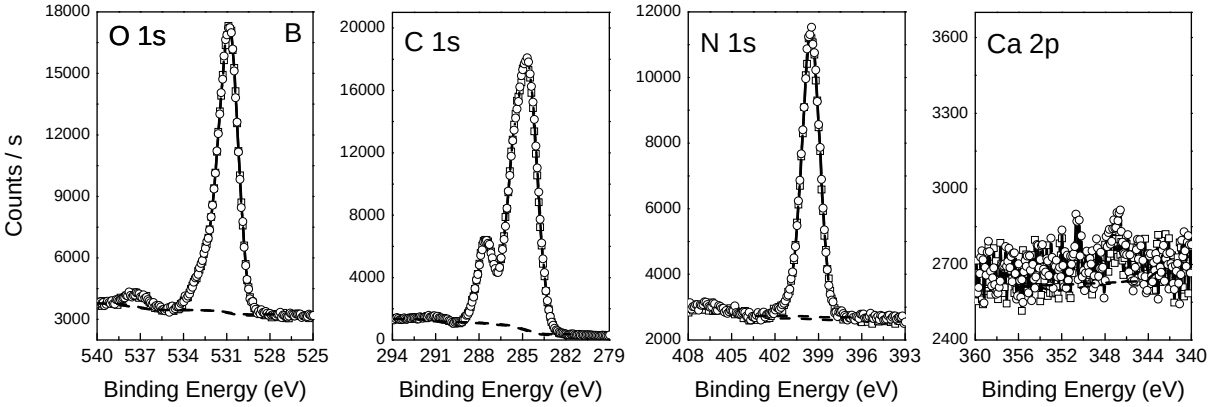
O 1s
B
C 1s
N 1s
Ca 2p
Counts / s
Binding Energy (eV)

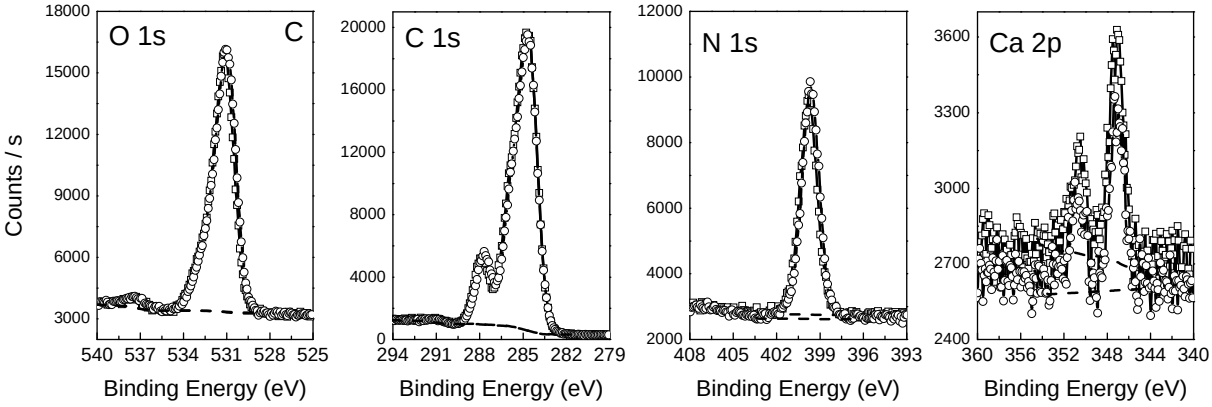
O 1s
C
C 1s
N 1s
Ca 2p
Counts / s
Binding Energy (eV)

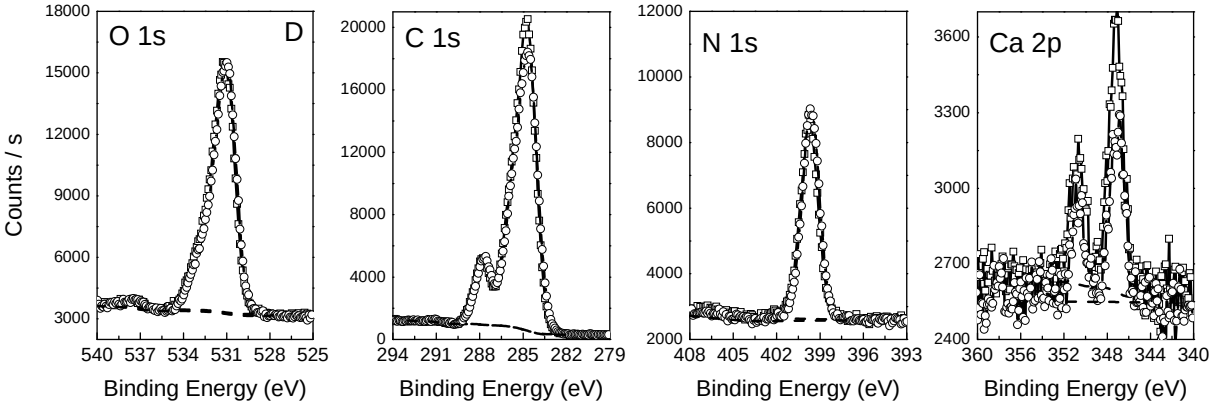
O 1s
D
C 1s
N 1s
Ca 2p
Counts / s
Binding Energy (eV)

Figure 5 Effect of calcium ions on zeta potential for NF90 and NF270 (A). High resolution XPS spectra (duplicate analysis) for NF270 exposed in Ca^{2+} solutions at different concentrations of 0 mM as control (B), 0.1 mM (C), and 1 mM (D). The minor Ca peak for the control membrane was caused by the 0.001 mM $CaCl_2$ rinse solution. The error bars represent the range based on two independent experiments.

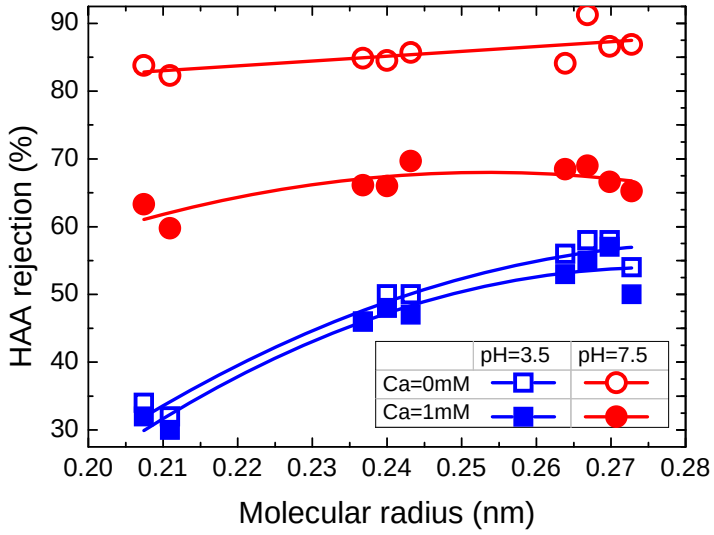

Figure 6 HAA rejection as a function of molecular radius at pH 3.5 and 7.5 in the presence of calcium ions by NF270.